Comb Copolymer Brush with Chemically Different Side Chains

Roman Stepanyan,*,† Andrei Subbotin,†,‡ and Gerrit ten Brinke†

Laboratory of Polymer Chemistry and Materials Science Center, University of Groningen, Nijenborgh 4, 9747 AG, Groningen, The Netherlands, and Institute of Petrochemical Synthesis, Russian Academy of Sciences, Moscow 117912, Russia

Received August 13, 2001; Revised Manuscript Received March 25, 2002

ABSTRACT: An investigation of side chain microphase separation within a single comb copolymer molecule containing chemically different A and B side chains has been carried out. Expressions for the transition point χ^*_{AB} in a good ($\chi^*_{AB} \sim N^{-3/8}$), marginal ($\chi^*_{AB} \sim N^{-1/2}$), θ ($\chi^*_{AB} \sim N^{-2/3}$), and poor ($\chi^*_{AB} \sim N^{-1}$) solvent are derived both by a mean field calculation and by scaling arguments. Properties of the system below and above the transition point are described. Some unusual "bowlike" conformations are predicted for a single molecule in the microphase separated state in a good solvent.

I. Introduction

The conformational characteristics of individual comb copolymers with a high grafting density of side chains in solution have been addressed in a series of theoretical papers[1−8] beginning with the original work of Birshtein et al.[1] Irrespective of the solvent quality, be it a good solvent or a θ solvent, all theories predict a cylindrical brushlike structure for sufficiently long side chains. The pertinent parameters are the side chain grafting density, the side chain length, the intrinsic stiffness of the backbone and the side chains (their respective Kuhn segments), and the solvent quality with respect to the side chains and the backbone. The conformation is characterized by a number of quantities, the persistence length of the comb copolymer brush being most important. For sufficiently long side chains the persistence length is predicted to exceed the backbone length, thus resulting in a characteristic cylindrical "bottle-brush" structure. Subsequent computer simulations using a freely jointed hard sphere model essentially confirmed this picture.[9−14]

The experimental investigation of comb copolymers with a high grafting density has assumed large proportions after the successful polymerization of macromonomers, yielding degrees of polymerization significantly exceeding the length of the macromonomer itself, by Tsukahara and co-workers.[15−18] Besides polymerization of macromonomers, alternative routes have been developed recently using grafting from a macroinitiator prepared by either atom transfer radical polymerization[19] or living cationic polymerization.[20] Using atom transfer radical polymerization, molecular brushes with block copolymer side chains have been prepared as well.[21]

The experimental characterization of the comb copolymer brush conformation in dilute solution is a highly nontrivial issue. It was achieved recently by Schmidt and co-workers[21−28] using a combination of light scattering experiments and theoretical modeling. Since the high grafting density is supposed to lead to a stiff molecular structure, the modeling has been based on the Kratky−Porod wormlike chain model. For high molar mass polymacromonomers based on methacryloyl end-functionalized oligo methacrylates (M_n = 2410 g/mol) in the good solvent THF, the Kuhn statistical segment length, which is twice the persistence length, turned out to be 120 nm. For polymacromonomers (M_n = 3624 g/mol) consisting of polystyrene main and side chains, this value was 190 nm in the good solvent toluene and 120 nm in the "θ solvent" cyclohexane.

One of the most challenging problems in polymer physics is the description of microphase separation in copolymer systems. Theoretically, self-organization in block copolymer systems has attracted a lot of attention during the past decades, and a fairly complete picture has emerged for the relatively simple diblock copolymers.[29−32] As a consequence, the interest gradually shifts toward more complicated architectures such as comb or graft copolymers.[33−37] The discussion of structure formation in comb copolymers using the weak segregation limit has been presented in some detail. Compared to diblock copolymers, the description is only slightly complicated by the fact that the single chain correlation functions are more involved. Phase diagrams of various comb copolymer systems have been published. Although different in details, the general trends are the same as for diblock copolymers. Of course, rather than the overall chain length, it is the length of the "repeat unit" that determines the order−disorder transition temperature as well as the characteristic length scale of the ordered structures.

The application of the weak segregation approach, however, requires a relatively low grafting density such that the distance between two consecutive grafting points along the backbone is at least of the order of the Flory radius of the side chains. If the grafting density of comb copolymers is very high, the structure in the melt will usually involve segregation between individual molecules. Even if the incompatibility between backbone and side chains is high, the high grafting density may well prevent segregation of several backbones. Furthermore, a high grafting density combined with long side chains implies the volume fraction of the backbone to be of the order of 0.1 or lower, not necessarily the most interesting part of the melt phase diagram.

Still, microphase separation may occur provided chemically different side chains are used. In this case

* To whom correpondence should be addressed. E-mail: R.R.Stepanyan@chem.rug.nl.
† University of Groningen.
‡ Russian Academy of Sciences.

10.1021/ma011441l CCC: $22.00
Published on Web 06/04/2002

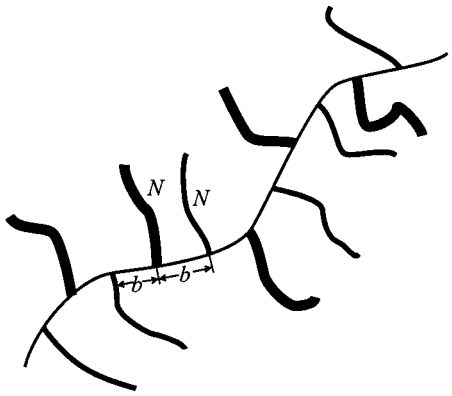

Figure 1. Schematic representation of a comb copolymer molecule. Thick and thin lines represent two chemically different side chains.

unfavorable interactions between the side chains may lead to a microdomain structure within a single molecule. The present paper is devoted to this subject. The main objective is to identify conditions for "microphase separation" of side chains of two different types within a single comb copolymer molecule under different solvent conditions.

The paper is organized as follows. The next section describes the self-consistent-field approach to a molecule with a *straight* backbone and chemically different side chains. We show the possibility of side chain separation within the molecule and discuss the limits of the theory's applicability. The subsequent section is devoted to possible unusual behavior of comb copolymer molecules with a *flexible* backbone and *microphase-separated* side chains. Then all results are summarized and discussed in the last section.

II. Straight Molecule with Two Types of Side Chains

Chemically different polymeric chains, namely of the type "A" and "B", are attached to a main chain with grafting density $1/b$. For simplicity, we choose the different side chains alternatingly grafted to the backbone so that the linear density of A (and B)-type chains is $^1/_2 b$ (Figure 1). Furthermore, we assume that the side chains have the same length $N_A = N_B \equiv N$ and statistical segment length a. Although the calculations can be done for arbitrary values of these quantities, we restrict ourselves to this simpler case in order to reduce the number of free parameters in the model.

To attain the cylindrical brush regime, the Flory radius of the side chain R_F should strongly exceed the distance b between two consecutive grafting points. This condition can always be fulfilled by choosing long enough side chains so that a cylindrical (i.e., straight) conformation will be realized. Therefore, we first consider a molecule with a straight backbone. Possible deviations from this conformation will be discussed further on.

To describe the interactions between the side chains and the solvent, we need a set of three parameters $v_{\alpha\beta}$ (α, β = A, B), which are directly related to the experimentally measured Flory−Huggins χ-parameters (χ_{AS}, χ_{BS}, χ_{AB}; see Appendix). As far as we are interested in the properties of the cylindrical brush induced by the side chains, we neglect any influence of the backbone.

Before presenting our calculations, we discuss first what kind of effects might be expected. Let us start from

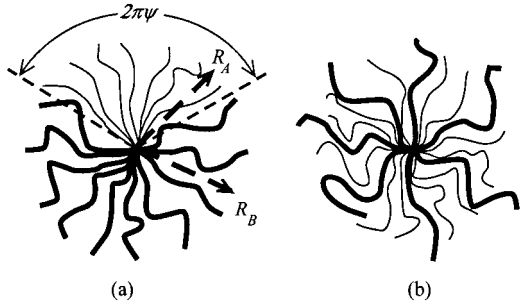

Figure 2. Cross section of the molecule: (a) in the separated state; (b) in the mixed state.

a molecule in a dilute solution in a solvent that is equally good for both species with the additional condition that A chains do not feel the presence of B chains in any other way than they feel the other A chains (repulsion between A and A, B and B, A and B is of the same strength). Therefore, they are both homogeneously distributed in the cross section of the brush molecule (Figure 2b; case $R_A \simeq R_B$ will be considered throughout the paper). With a gradual increase of the A−B (repulsive) interaction parameter, chains of different nature try to avoid each other, but they are still mixed due to a certain entropic threshold. However, beyond some value v^*_{AB} one can expect a transition manifesting itself in the separation of A chains from B chains within the comb copolymer molecule (Figure 2a). This point v^*_{AB} can be estimated by comparing the free energies of the mixed F_{mix} and the separated F_{sep} states calculated on the basis of the side chain density distribution in the cross section of the molecule. Of course, this will not give us the exact binodal point (in reality, the transition will be smoother than assumed here) but rather a good estimation knowing that this method gives an almost exact result in the case of diblock copolymers.[30,38]

A. SCF Approach. The free energy in the straight brush regime (assuming a straight backbone) can in the most general form be written as

$$F = F_{conf,A} + F_{conf,B} + F_{int} \tag{1}$$

The interaction part of the free energy F_{int} per chain in the second virial approximation has the simple form

$$F_{int} = \frac{b}{2}\int_0^{2\pi} d\varphi \int_0^{\infty} r\, dr \sum_{\alpha,\beta} v_{\alpha\beta} c_\alpha(r,\varphi)\, c_\beta(r,\varphi) \tag{2}$$

Here we use the polar coordinate system with the z-axis pointing along the straight backbone and measure the free energy in the units of $k_B T$ (this makes *all* quantities with the dimension of energy dimensionless in the present paper); $c_\alpha(r,\varphi)$ are the concentration profiles (α, β = A, B). The conformational free energy of a type α chain $F_{conf,\alpha}$ corresponds to the free energy of a stretched Gaussian chain[5,39,40]

$$F_{conf,\alpha} = b\int_0^{2\pi} d\varphi \int_0^{\infty} r\, dr\, [-g_\alpha(r,\varphi) \ln Z_\alpha(r,\varphi;N \mid \mu_\alpha) - \mu_\alpha(r,\varphi)\, c_\alpha(r,\varphi) + g_\alpha(r,\varphi) \ln g_\alpha(r,\varphi)] \tag{3}$$

where some new functions have been introduced. Z_α is a partition function of a chain of length N with *two fixed ends* (one at the zero point and the other at (r,φ)) in the external field μ_α, so that $-\ln Z_\alpha$ is the corresponding free energy. To take into account the distribution of the side chain's free end, one should average the energy $-\ln$

Z_α with a distribution function of the free end $g(r,\varphi)$ and add the translational entropy term $g \ln g$. The expression for the free energy eq 3 can be easily verified in the *limiting case of an ideal chain*[39] when $\mu = 0$ and $-\ln Z_\alpha = 3r^2/(2Na^2)$ so that minimization with respect to g gives $g = C \exp(-3r^2/2Na^2)$, where C is a normalization constant.

Following ref 5, we employ an analogy between a stretched Gaussian chain whose partition function is to be found from a Schrödinger type equation[39,41] (t enumerates monomeric units)

$$\frac{\partial Z(r,\varphi;t|\mu)}{\partial t} = \frac{a^2}{6}\Delta Z(r,\varphi;t|\mu) - \mu(r,\varphi)\, Z(r,\varphi;t|\mu) \quad (4)$$

and a quantum particle moving in the field μ. Using this analogy with the well-known semiclassical WKB approximation, one obtains the partition function in the form

$$Z = \mathrm{e}^{-tE-S(r)} \quad (5)$$

where $S(r) \simeq (\sqrt{6}/a)\int_0^r \mathrm{d}r_1\, [\mu(r_1) - E]^{1/2}$ and E is the analogy of the particle's energy, which will be implicitly calculated further on (for details see ref 5).

All the other functions in eqs 2 and 3 (c_α, μ_α, g_α) have to be determined from the free energy eq 1 extremum. This requires some additional assumptions about the side chain alignment structure around the backbone.

1. Separated State. Suppose the A−B "repulsion" parameter v_{AB} is large enough and the system has already undergone side chain separation. This means that A-type side chains are concentrated inside some angle $2\pi\psi$ ($0 < \psi < 1$) as depicted in Figure 2a, and the number of B side chains in this region is exponentially small

$$c_A(r,\varphi) = \begin{cases} c_A(r) & -\pi\psi < \varphi < \pi\psi \\ 0 & \text{otherwise} \end{cases} \quad (6)$$

The analogous fact is true for the B-type side chains in the other part of the angle space $\pi\psi < \varphi < 2\pi - \pi\psi$.

Additionally, we will use the Alexander−de Gennes approximation[41] for the free end distribution functions implying that all A-chains' free ends are located in some very narrow region near R_A (and R_B for B chains)

$$g_\alpha = \frac{1}{4\pi\psi_\alpha b}\frac{\delta(r - R_\alpha)}{r} \quad (7)$$

The numerical prefactor in eq 7 follows from the normalization condition. The functions c_A and c_B have to be normalized as well: $4\pi\psi b \int_0^{R_A} r\, \mathrm{d}r\, c_A(r) = N$ and $4\pi(1 - \psi)b\int_0^{R_B} r\, \mathrm{d}r\, c_B(r) = N$.

Equations 6 and 7 together with the partition functions Z_α taken in the form eq 5 significantly simplify the free energy for the separated state

$$F_{sep} = \frac{N}{2}(E_A + E_B) - \frac{1}{2}\ln\psi - \frac{1}{2}\ln(1-\psi) + \frac{\sqrt{6}}{2a}\sum_{\alpha=A,B}\int_0^{R_\alpha}\mathrm{d}r\,\sqrt{\mu_\alpha(r) - E_\alpha} + 2\pi b\sum_{\alpha=A,B}\psi_\alpha\int_0^{R_\alpha} r\,\mathrm{d}r\left(-\mu_\alpha(r)\, c_\alpha(r) + \frac{1}{2}v_{\alpha\alpha}c_\alpha^{\,2}(r)\right) \quad (8)$$

Here $\psi_A \equiv \psi$ and $\psi_B \equiv 1 - \psi$, and the energy of the A−B interface is neglected (consistency of this assumption will be verified further on). Together with eq 8, the self-consistency condition $\delta F_{sep}/\delta c_\alpha = 0$ should be fulfilled. This gives the following relation between the concentration and the chemical potential

$$c_\alpha = \frac{\mu_\alpha}{v_{\alpha\alpha}} \quad (9)$$

As the next step, functions μ_A and μ_B should be obtained from the extremum condition of eq 8. Note that the minimum of the free energy as a function of concentration implies a maximum as a function of the chemical potential as a conjugated variable.[5] Taking into account relation eq 9, we arrive at the equation for the chemical potentials

$$\frac{\sqrt{6}}{4a}\frac{v_{\alpha\alpha}}{\sqrt{\mu_\alpha(r) - E_\alpha}} = 2\pi br\psi_\alpha\mu_\alpha(r) \quad (10)$$

which together with the normalization condition for the concentration rewritten in the form

$$\frac{4\pi\psi_\alpha b}{Nv_{\alpha\alpha}}\int_0^{R_\alpha} r\,\mathrm{d}r\,\mu_\alpha(r) = 1 \quad (11)$$

gives the complete set of equations for E_α and $\mu_\alpha(r)$.

With reasonable accuracy, the solution of eq 10 can be approximated as[5]

$$\mu_\alpha(r) \simeq E_\alpha + \left(\frac{\sqrt{6}v_{\alpha\alpha}}{8\pi\psi_\alpha abr}\right)^{2/3} \quad (12)$$

Here E_A and E_B follow from the normalization eq 11.

In this way the free energy eq 8 becomes a function of three parameters R_A, R_B, and ψ and can be easily minimized. It leads to the following expressions for the radii of the comb copolymer cylindrical brush

$$R_A \simeq \frac{0.48}{\psi_0^{1/4}}\left(\frac{a^2v_{AA}N^3}{2b}\right)^{1/4}$$

$$R_B \simeq \frac{0.48}{(1-\psi_0)^{1/4}}\left(\frac{a^2v_{BB}N^3}{2b}\right)^{1/4} \quad (13)$$

where $2\pi\psi_0$ is the equilibrium value of the angle occupied by the A side chains in the cross section of the cylindrical molecule, which should be determined from the equation

$$\sqrt{\frac{15}{32\pi}}\left(\frac{N}{a^2b}\right)^{1/2}\left[\frac{v_{AA}}{\psi_0^{3/2}} - \frac{v_{BB}}{(1-\psi_0)^{3/2}}\right] = \frac{1}{1-\psi_0} - \frac{1}{\psi_0} \quad (14)$$

The free energy per side chain in this case reads

$$F_{sep} = 0.386\left(\frac{N}{a^2b}\right)^{1/2}\left[\sqrt{\frac{v_{AA}}{\psi_0}} + \sqrt{\frac{v_{BB}}{1-\psi_0}}\right] - \frac{1}{2}\ln[\psi_0(1-\psi_0)] \quad (15)$$

Equation 14 cannot be solved in the general case but obviously has a root $\psi_0 = {}^1/_2$ for $v_{AA} = v_{BB} \equiv v$. In this particular case the free energy eq 15 simplifies to

$$F_{sep}^{(1/2)} = 1.092\left(\frac{Nv}{a^2 b}\right)^{1/2} + \ln 2 \qquad (16)$$

This result coincides with the one obtained in ref 5 and is very similar to refs 42 and 43 except for the entropic ln 2 term, which is not present in the cited works due to the difference in the system studied.

Now let us estimate the thickness of the interface region. The typical blob size in the interpenetration region should have energy of the order of $1(k_B T)$. If it consists of g links, then its size may be estimated as $a\sqrt{g}$, and therefore the A−B interaction energy inside the blob reads

$$\frac{gv}{a^3 g^{3/2}}\, g\chi_{AB} \sim 1 \qquad (17)$$

To use expression eq 16 for the free energy in the vicinity of the transition point, we have to make sure that $g \ll N$. Together with eq17 this gives a condition for the eq16 applicability:

$$\chi_{AB} \gg \frac{a^3}{v}\frac{1}{\sqrt{N}} \qquad (18)$$

2. Mixed State. So far we have calculated the free energy of the comb copolymer molecule in the "separated" state. The same method can be applied to the "mixed" state of the system, where A and B side chains are homogeneously mixed, and therefore the concentration profiles have to be chosen in the form (α = A, B)

$$c_\alpha(r,\varphi) = c_\alpha(r), \quad 0 < \varphi < 2\pi \qquad (19)$$

Similar to the separated state eq 8, we can calculate the free energy F_{mix} in the framework of WKB and Alexander−de Gennes approximations

$$F_{mix} = \frac{N}{2}(E_A + E_B) + \frac{\sqrt{6}}{2a}\sum_{\alpha=A,B}\int_0^{R_\alpha} dr\,\sqrt{\mu_\alpha(r) - E_\alpha} + 2\pi b\sum_{\alpha=A,B}\int_0^{R_\alpha} r\,dr\left(-\mu_\alpha(r)\,c_\alpha(r) + \frac{1}{2}v_{\alpha\alpha}c_\alpha^{\,2}(r)\right) + 2\pi b\int_0^{\min(R_A;R_B)} r\,dr\; v_{AB}c_A(r)\,c_B(r) \qquad (20)$$

Note that the entropic logarithmic terms (see eq 8) are absent, and an integral responsible for the A−B interaction is added. Without loss of generality we further assume that $R_A \le R_B$ (but $R_A \simeq R_B$ still holds).

The computations happen to be a bit more complicated now because of the nontrivial relation between concentrations and chemical potentials (compare with eq 9)

$$c_A = \frac{\mu_A v_{BB} - \mu_B v_{AB}}{v_{AA}v_{BB} - v_{AB}^{\,2}}, \quad c_B = \frac{\mu_B v_{AA} - \mu_A v_{AB}}{v_{AA}v_{BB} - v_{AB}^{\,2}} \qquad (21)$$

This leads to a set of two third-order algebraic equations for the chemical potentials instead of eq 10, and the simple approximation eq 12 cannot be employed.

To simplify the equation, we note that all the difficulties disappear for the case of $v_{AA} = v_{BB} \equiv v$ considered at the end of the previous subsection. It gives chemical potentials (now $\mu_A(r) = \mu_B(r) \equiv \mu(r)$) in the form

$$\mu(r) \simeq E + \left(\frac{\sqrt{6}(v + v_{AB})}{8\pi abr}\right)^{2/3} \qquad (22)$$

where $E \equiv E_A = E_B$ and the concentration profile is coupled to $\mu(r)$ as $c(r) = (v + v_{AB})^{-1}\mu(r)$. The constants $E_{A,B}$ are found from the normalization of $c(r)$ and read

$$E_\alpha = \frac{Nv}{\pi b R_\alpha^{\,2}} - \frac{3}{2}\left(\frac{\sqrt{6}(v + v_{AB})}{8\pi abR_\alpha}\right)^{2/3} \qquad (23)$$

Finally, substituting eq 22 and eq 23 into the free energy eq 20 and minimizing, one obtains radii of the brush

$$R_{A,B} \simeq 0.48\left(\frac{a^2(v + v_{AB})N^3}{2b}\right)^{1/4} \qquad (24)$$

and the free energy

$$F_{mix}^{(1/2)} = 0.772\left(\frac{N(v + v_{AB})}{a^2 b}\right)^{1/2} \qquad (25)$$

As expected, the free energy increases with increasing strength of the A−B repulsion. The interaction between A and B side chains also renormalizes the numerical prefactor in comparison with eq 16.

3. Transition from Mixed to Separated State. At this point it is easy to estimate the value v_{AB}^* of the A−B interaction parameter *separating* mixed and segregated states. Comparing eq 16 to eq 25, one gets

$$v_{AB}^* = v + 2.5\left(\frac{a^2 bv}{N}\right)^{1/2} + 0.8\frac{a^2 b}{N} \qquad (26)$$

Keeping in mind that v and v_{AB} are effective parameters, we can use eq A3 from the Appendix to express this point in terms of the χ parameters ($\chi_{AS} = \chi_{BS} \equiv \chi$)

$$\chi_{AB}^* N = 0.8\frac{ba^2}{v} + 2.5\sqrt{\frac{Nba^2}{v}(1 - 2\chi)} \qquad (27)$$

Here v is the volume of one bead in the model. As follows from eq 27, only the second term is important well above the θ-point. The χ_{AB}^* parameter appears to be proportional to $N^{-1/2}$ as

$$\chi_{AB}^* \sim \frac{1}{\sqrt{N}} \qquad (28)$$

Comparing the result eq 27 with condition eq 18, one can see the interfacial term is indeed important at the transition region. This implies that SCF calculation generally should be conducted incorporating compositional inhomogeneity effects into the free energy. Nevertheless, the result eq 28 still holds giving correct scaling prediction for the transition point.

Now let us address the problem of the mean field approach applicability. The method itself implies that fluctuations are small. Thus, we have to apply the result eq 28 rather to a marginal than to a "very good" solvent. It is also possible to estimate a range of parameters where all assumptions, made before, are fulfilled. First of all, note that the second virial approximation that we use is valid for small concentrations when additionally the second virial term is dominant over the third one, i.e., according to eq A2 for $1 - 2\chi > vc$ or

$$1 - 2\chi > \left(\frac{\nu}{ba^2}\right)^{1/3} N^{-1/3} \tag{29}$$

On the other hand, the mean field approach is correct if the correlation volume contains many different chains; otherwise, one should use the renormalization group method[44−46] in order to describe the situation in a consistent way. The correlation radius of the brush is of the order of[39]

$$\xi \sim \frac{a}{\sqrt{c\nu(1-2\chi)}} \sim a\left(\frac{ba^2}{\nu}\right)^{1/4} \frac{N^{1/4}}{(1-2\chi)^{1/4}} \tag{30}$$

Therefore, the segments' concentration in the blob of the size ξ is

$$c_0 \sim \frac{g(\xi)}{\xi^3} \sim \frac{1}{a^2\xi} \tag{31}$$

This concentration should be less than the average concentration c inside the brush, $c_0 < c$, which also implies that the correlation volume contains many thermal blobs. The last inequality yields

$$1 - 2\chi < \left(\frac{a}{b}\right)^{4/3}\left(\frac{ba^2}{\nu}\right)N^{-1/3} \tag{32}$$

The range of the parameter values satisfying eqs 29 and 32 corresponds to the "marginal semidilute region" in the terminology of Schaefer et al.[47]

Thus, using eqs 29 and 32, we find that the mean field approach can be applied if $\nu/a^3 \ll 1$, i.e., for chains with a large Kuhn segment.

Finally, note that the situation under θ conditions can be considered using the scheme above starting from eq 1 with the interaction part including the third virial coefficients

$$F_{\text{int}}^{(\theta)} = \frac{1}{6}w\sum_{i=0}^{3} c_{\text{A}}^{i} c_{\text{B}}^{3-i} + v_{\text{AB}}c_{\text{A}}c_{\text{B}}$$

The result for the transition point is

$$\chi_{\text{AB}}^{*} N \sim N^{1/3}$$

The exponent in this scaling law is less than that for the marginal solvent eq 27.

4. Straight Molecule in a Poor Solvent. Having described the comb copolymer molecule in a good solvent, we now turn to the case of a poor solvent. One can argue that even for high grafting densities the straight brush regime may be inaccessible under poor solvent conditions. Nevertheless, we will restrict ourselves to the straight conformation of the molecule assuming the backbone to be a quite stiff persistent chain.

Basically the same approach can be used except for the expression for the interaction energy eq 2. Under poor solvent conditions solvent molecules practically do not penetrate inside the side chains corona around the backbone. This means that eq 2 should be modified accordingly

$$F_{\text{int}} = \int_0^{2\pi}\int_0^{\infty} r\,\mathrm{d}r\; \nu\chi_{\text{AB}} c_{\text{A}}(r,\varphi)\, c_{\text{B}}(r,\varphi) \tag{33}$$

which resembles more the melt situation.

Separated State. Assuming as before that ψ part of the angle space is occupied by A chains and using the normalization condition for $c_{\text{A}}(r,\varphi)$ given in the form

$$c_{\text{A}}(r,\varphi) = \begin{cases} c_{\text{A}} & -\pi\psi < \varphi < \pi\psi,\ r_0 < r < R_{\text{A}} \\ 0 & \text{otherwise} \end{cases} \tag{34}$$

where c_{A} = constant and r_0 is some cutoff parameter (corresponding to the radius of the backbone), one gets

$$c_{\text{A}} = \frac{N}{2\pi\psi b R_{\text{A}}^{\,2}} \tag{35}$$

The radius R_{A} follows from the incompressibility condition $c_{\text{A}} = 1/\nu$ as

$$R_{\text{A}} = \left(\frac{N\nu}{2\pi\psi b}\right)^{1/2} \tag{36}$$

The free energy as a functional of the chemical potentials and concentrations can be written in a form very similar to eq 8

$$F'_{\text{sep}} = \frac{N}{2}(E_{\text{A}} + E_{\text{B}}) - \frac{1}{2}\ln\psi - \frac{1}{2}\ln(1-\psi) + \sum_{\alpha=\text{A,B}}\left(\frac{\sqrt{6}}{2a}\int_{r_0}^{R_\alpha}\mathrm{d}r\,\sqrt{\mu_\alpha(r) - E_\alpha} - 2\pi\psi_\alpha b\int_{r_0}^{R_\alpha} r\,\mathrm{d}r\,\mu_\alpha(r)c_\alpha\right) \tag{37}$$

Here we used again the WKB and Alexander−de Gennes approximations. Despite the fact that the situation in a poor solvent is more similar to a melt than to the good solvent condition, we can still employ the Alexander−de Gennes approximation. (The high grafting density still ensures strong stretching of the side chains.) In contrast to eq 8, the only free functions in eq 37 are μ_{A} and μ_{B}. They follow from $\delta F'/\delta\mu_\alpha = 0$ and have the form

$$\mu_\alpha(r) = E_\alpha + \frac{3}{8}\frac{R_\alpha^{\,4}}{a^2N^2r^2} \tag{38}$$

Substituting eqs 35, 36, and 38 into the free energy eq 37, $\psi = {}^1/_2$ is found from the minimization. As a result, the free energy reads

$$F'_{\text{sep}} = \frac{3\nu}{8\pi a^2 b}\ln\frac{N\nu}{\pi b r_0^{\,2}} + \ln 2 \tag{39}$$

The parameter r_0, which has been introduced to avoid singularities in the free energy, corresponds to the bare backbone radius and can be estimated as $r_0 \simeq b$.

Mixed State. We now consider a homogeneous mixture of A and B chains inside the region of radius R_{A} around the backbone. Using the same arguments as before, one obtains the concentrations

$$c_{\text{A}} = c_{\text{B}} = \frac{N}{2\pi b R_{\text{A}}^{\,2}} \tag{40}$$

and radius of the brush

$$R_{\text{A}} = \left(\frac{N\nu}{\pi b}\right)^{1/2} \tag{41}$$

which have to be plugged into the free energy

$$F'_{\mathrm{mix}} = \frac{N}{2}(E_{\mathrm{A}} + E_{\mathrm{B}}) + 2\pi b\nu \int_{r_0}^{R_{\mathrm{A}}} r\, \mathrm{d}r\, \chi_{\mathrm{AB}} c_{\mathrm{A}} c_{\mathrm{B}} + \sum_{\alpha=\mathrm{A,B}} \left(\frac{\sqrt{6}}{2a} \int_{r_0}^{R_\alpha} \mathrm{d}r\, \sqrt{\mu_\alpha(r) - E_\alpha} - 2\pi b \int_{r_0}^{R_\alpha} r\, \mathrm{d}r\, \mu_\alpha(r) c_\alpha \right) \tag{42}$$

Following the same procedure as before, we end up with the free energy for the mixed state

$$F'_{\mathrm{mix}} = \frac{3\nu}{8\pi a^2 b} \ln \frac{N\nu}{\pi b r_0^{\,2}} + \frac{N}{4}\chi_{\mathrm{AB}} \tag{43}$$

Transition Point. Now we are ready to compare free energies eq 39 and eq 43 to obtain the transition point χ^*_{AB}. In the case of a poor solvent χ^*_{AB} is completely determined by the entropy threshold

$$N\chi^*_{\mathrm{AB}} = 4 \ln 2 \simeq 2.8 \tag{44}$$

Of course, the consideration above is valid in the framework of the assumption about approximately circular shape of the molecule's cross section, providing the smallest possible area of the contact with the solvent. This obviously implies a very poor solvent for both species.

The above result has a form which is typical for theories of microphase separation in melts,[30,31,36] but the numerical value is somewhat smaller. It is quite easy to understand: the entropy loss due to the constraining motion of only one end of the side chain to get the segregated structure (the second one is fixed anyway in the grafting point) is much less than the loss of the translational motion entropy, for instance, of a diblock molecule restricted to be inside the domain (micelle, lamella, etc.).

B. Scaling Approach—Good Solvent. At the end of this section we show how to estimate the critical χ^*_{AB} parameters using simple scaling arguments. The transition point from the mixed to the separated state can be found from the condition that the energy of the A−B contacts per side chain ΔE is of the order of $k_{\mathrm{B}}T$, $\Delta E \sim 1(k_{\mathrm{B}}T)$. This energy is given by

$$\Delta E \sim N p(\phi) \chi_{\mathrm{AB}} \tag{45}$$

Here $p(\phi)$ is the probability of the A−B contact, which depends on the average volume fraction ϕ of the monomers inside the brush. According to the mean field approach, $p(\phi) \simeq \phi$ where

$$\phi \sim \nu N/(bR^2) \tag{46}$$

and R is the radius of the brush. The last one is proportional to $N^{3/4}$ for a marginal solvent, eq 24, $N^{2/3}$ for a θ solvent (see ref 1, for instance), and $N^{1/2}$ for a poor solvent. Applying formula eq 45 for each of these three cases, we obtain as scaling law for a marginal solvent

$$\chi^{*(\mathrm{m})}_{\mathrm{AB}} \sim N^{-1/2} \tag{47}$$

for a θ solvent

$$\chi^{*(\theta)}_{\mathrm{AB}} \sim N^{-2/3} \tag{48}$$

and for a poor solvent

$$\chi^{*(\mathrm{poor})}_{\mathrm{AB}} \sim N^{-1} \tag{49}$$

Clearly, all three results eqs 47−49 are consistent with the mean-field calculations presented in the previous subsections.

However, the situation is different for a good solvent. The probability of contact in this case is smaller and is given by[39,41]

$$p(\phi) = \phi^{5/4} \sim N^{-5/8} \tag{50}$$

Note, here we used an equation for the radius of the brush in good solvent $R \sim N^{3/4}$ (see ref 1). Hence, using eq 45, we find that the critical point for a good solvent is

$$\chi^{*(\mathrm{good})}_{\mathrm{AB}} \sim N^{-3/8} \tag{51}$$

III. Bending Effects: SCF Approach

In this section we relax the straight backbone constraint and generalize the approach to calculate the free energy of a bent comb copolymer molecule. Our goal is to obtain the free energy as a series in the small parameter $1/R$, where R is the radius of the backbone's curvature. According to refs 48 and 49 in the absence of the linear term in the expansion, the persistence length of the molecule is determined by the second-order term (the 0th term corresponds to the straight comb). This is the normal situation for a symmetrical system where the persistent bending mechanism works.

However, for an asymmetric molecule (such as a microphase-separated brush) the linear term in the expansion is responsible for the presence of a spontaneous curvature leading to the stability of bent conformations. Similar effects in two-dimensional conformations of "simple" molecular bottle-brushes have attracted considerable attention recently.[7,8,26,50]

Let us consider therefore a bent comb molecule with completely separated side chains (i.e., *far* above χ^*_{AB} transition point). General ideas about how to construct the free energy functional for this case can be found in ref 5. We follow the same approach and introduce a new set of functions for the perturbed (i.e., bent) state of the molecule

$$c^*_\alpha(r,\varphi) = c_\alpha(r) + \delta c_\alpha(r,\varphi)$$

$$\mu^*_\alpha(r,\varphi) = \mu_\alpha(r) + \delta\mu_\alpha(r,\varphi)$$

$$E^*_\alpha(\varphi) = E_\alpha + \delta E_\alpha(\varphi)$$

$$g^*_\alpha(r,\varphi) = \begin{cases} (\theta_\alpha(\varphi)/4\pi\psi br)\delta(r - R_\alpha) & -\pi\psi < \varphi < \pi\psi \\ 0 & \text{otherwise} \end{cases} \tag{52}$$

Here a system of coordinates has been introduced with z-axis along the backbone; (r,φ) are polar coordinates in the cross section; E_α, c_α, and μ_α are given by the expressions for the straight backbone.

Note that the free end distribution function is now written in the form of the perturbed Alexander−de Gennes approximation. This correction $\theta_\alpha(\varphi)$ can be found from the self-consistency equation

$$\theta_\alpha(\varphi) = B_\alpha c^*_\alpha(R_\alpha,\varphi) \tag{53}$$

with constants B_α (α = A, B).

Employing the WKB approximation, one can write the free energy of the bent cylindrical brush molecule in the form $F^* = F_A^* + F_B^*$

$$F_A^* = \frac{1}{4\pi\psi}\int_{-\pi\psi}^{\pi\psi} d\varphi \left(1 + \frac{R_A \cos\varphi}{R}\right)\theta_A(\varphi)\left[N_A E_A^*(\varphi) + \frac{\sqrt{6}}{a}\int_0^{R_A} dr\, \sqrt{\mu^*(r,\varphi) - E^*(\varphi)} + \ln\frac{\theta_A(\varphi)}{\psi}\right] + 2\pi b\psi \int_0^{R_A} r\, dr \left(1 + \frac{r\cos\varphi}{R}\right)\left(-\mu_A^*(r,\varphi)\, c_A^*(r,\varphi) + \frac{v_{AA}}{2} c_A^{*2}(r,\varphi)\right) \quad (54)$$

and similar for F_B^*.

Using the self-consistency condition for the concentration c_α^* in the form of eq 9, the chemical potential has to be found from the equation

$$\frac{\sqrt{6}}{4a}\frac{v_{AA}}{\sqrt{\mu_A^*(r,\varphi) - E_A^*(\varphi)}} = \frac{2\pi\psi}{\theta_A(\varphi)}\, br\, \frac{1 + \frac{r\cos\varphi}{R}}{1 + \frac{R_A\cos\varphi}{R}}\, \mu_A^*(r,\varphi) \quad (55)$$

which is solved according to the perturbation scheme eq 52.

Omitting the details of the calculation, we give the result for the corrections to the free energy due to the bending.

$$F^* = F_0 + \frac{F^{(I)}}{R} + \frac{F^{(II)}}{R^2}$$

$$F^{(I)} \simeq -0.004\left(\frac{N^5}{a^2 b^3 v}\right)^{1/4}\Delta v$$

$$F^{(II)} \simeq 0.1\frac{N^2 v}{b} \quad (56)$$

Here we give only the main corrections to the straight brush free energy F_0, assuming $\Delta v = v_{BB} - v_{AA}$ to be small. As one can see, the straight conformation is no longer favorable, and a spontaneous curvature $R_0 = -2F^{(II)}/F^{(I)}$ will occur. An estimation of R_0 from eq 56 gives

$$R_0 \simeq 62\left(\frac{a^2 v N^3}{b}\right)^{1/4}\frac{v}{\Delta v} \quad (57)$$

Finally, rewriting eq 57 in terms of χ parameters results in

$$R_0 \sim \frac{(1-2\chi)^{5/4}}{\Delta\chi} N^{3/4} \quad (58)$$

Of course, eq 58 is valid well above the θ point in the good solvent regime. In principle, the same derivation can be done under θ conditions by introducing the third virial coefficient.

Qualitatively, eq 57 can be obtained from simple arguments, too. Indeed, upon bending the cylinder corresponding to the straight comb molecule gets distorted and assumes a toroid shape. This implies that the volume of the A chains occupying the outer part (we assume $\psi \simeq 1/2$) of the torus is (corresponding to a unit of the length b along the backbone)

$$V_{out} = b\left(\frac{\pi R_A^{\,2}}{2} + \frac{2R_A^{\,3}}{3R}\right) \quad (59)$$

and similarly for the inner (occupied by B) part, but with the second term subtracted.

Knowing that the free energy has to scale as

$$F \sim v_{AA} V_{out} c_A^{\,2} + v_{BB} V_{in} c_B^{\,2} \quad (60)$$

with concentrations $c_A \sim N/V_{out}$ and $c_B \sim N/V_{in}$, one finally obtains

$$\frac{F^*}{F_0} \sim 1 + \frac{v_{BB} - v_{AA}}{v_{BB} + v_{AA}}\frac{R_A}{R} + \frac{R_A^{\,2}}{R^2} \quad (61)$$

Now it is easy to see from the minimization of eq 61 that the spontaneous curvature scaling law is

$$R_0 \sim R_A \frac{v}{\Delta v} \quad (62)$$

which coincides with eq 57.

In the closure of the present section we would like to emphasize that the spontaneous curvature eq 58 in the present model is the result of an interaction between *nearest* neighbors (compare to ref 51 where toroidal shape of the conformation is the result of an attraction between neighbors that are *far apart*, causing a coil−globule transition). In some sense our situation resembles the one considered in ref 50 for 2D, where asymmetry of adsorbed comb copolymer conformations was claimed to be caused by stochastic processes during the adsorption. On the contrary, in our case the curvature eq 58 is an *intrinsic* property of the molecule in the separated state, and the only reason for it is the difference in the interaction parameters χ_{AS} and χ_{BS} of two chemically different species with the solvent.

IV. Concluding Remarks

In the present paper we considered a comb copolymer molecule with two types of side chains attached to a common backbone. We found that the spatial separation of the side chains within the molecule is possible if the A−B interaction parameter takes values larger than a predicted χ_{AB}^*. This point has been calculated as a function of the solvent quality resulting in the following scaling laws

$$\chi_{AB}^* N \sim N^{5/8} \quad \text{good solvent}$$

$$\chi_{AB}^* N \sim N^{1/2} \quad \text{marginal solvent}$$

$$\chi_{AB}^* N \sim N^{1/3} \quad \theta \text{ solvent}$$

$$\chi_{AB}^* N \sim 1 \quad \text{poor solvent}$$

The exponent value gradually decreases from $5/8$ to 0 when going from good to poor solvent conditions. The result for a poor solvent is typical for all microphase separation theories in melts.[30,31,36] It should be possible to observe the described phenomena in an experiment choosing the appropriate length of the side chains, because χ_{AB}^* scales as $N^{-3/8}$ under good solvent condi-

tions, and hence, small positive values of the χ_{AB} parameter can already lead to the transition.

In the present work we considered a comb molecule with alternating chemically different side chains. In many cases the synthetic procedure will lead to chemically different side chains distributed statistically along the backbone. The appearance of large groups of "like" chains is then possible, which may change the separation picture drastically: a separation along the backbone may occur rather than in the cross section. But, if the statistical distribution of the side chains is so that formation of the large groups (containing about R_F/b side chains) is improbable, then the obtained results remain valid at least qualitatively.

It would be interesting to look at the system in a selective solvent (for instance, good for A and poor for B). In the "mixed" state, one can expect to find highly stretched A side chains and B chains collapsed onto the backbone. For large enough χ_{AB} (corresponding to the "separated" state), one can expect the formation of even more peculiar shapes: for example, the B chains can form a dense cylinder twined by the backbone with A side chains pointing radially into the solvent. Of course, this system is out of the scope of this work in the sense that the methods, and the approximations used will not be valid in that region. (It was assumed throughout that the radii of A and B brushes are close to each other.)

In the previous section we described the comb copolymer molecule in the separated state. It was shown that a spontaneous curvature

$$R_0 \sim \frac{N^{3/4}}{\Delta\chi}$$

should occur as a result of the difference in the osmotic pressures in the spatially separated A and B phases. In the our model the χ parameters were responsible for the bending, but in principle, the same effect can be achieved if other characteristics (molecular weight, grafting density) of the A and B side chains differ.

Acknowledgment. The authors are pleased to acknowledge R. J. Nap for discussion of peculiarities of the microphase separation in the weak segregation limit and Prof. I. Erukhimovich and Prof. S. Kuchanov for interesting remarks concerning this work. Also, the anonymous referees, whose critical remarks allowed us to improve the quality of the paper, are acknowledged.

Appendix: Relation between ν Interaction Parameters and Flory−Huggins χ Parameters

Interaction parameters $\nu_{\alpha\beta}$ (α, β = A, B) used in the current work have the meaning similar to the second virial coefficients in pair A−A, B−B, and A−B interactions. They can be easily related to Flory−Huggins χ parameters for polymer−solvent χ_{AS}, χ_{BS} and polymer−polymer χ_{AB} interactions. In the framework of the Flory approach the mixing energy should be written[41] in the form ($k_BT \equiv 1$)

$$E_{\text{mixing}} = \int_V \frac{dV}{\nu}[\Phi_S \ln \Phi_S + \chi_{AS}\Phi_A\Phi_S + \chi_{BS}\Phi_B\Phi_S + \chi_{AB}\Phi_A\Phi_B] \quad \text{(A1)}$$

Here Φ_α denotes the specific volume occupied by α component (A polymer, B polymer, or solvent); ν represents the volume of the monomeric unit (bead).

Substituting the incompressibility condition

$$\Phi_S = 1 - \Phi_A - \Phi_B$$

and expanding eq A1 one gets (omitting constants and terms linear in Φ_A and Φ_B)

$$E_{\text{mixing}} = \int_V \frac{dV}{\nu}\left[\frac{1}{2}(1 - 2\chi_{AS})\Phi_A^2 + \frac{1}{2}(1 - 2\chi_{BS})\Phi_B^2 + (1 + \chi_{AB} - \chi_{AS} - \chi_{BS})\Phi_A\Phi_B\right] \quad \text{(A2)}$$

Knowing that $\Phi_\alpha = \nu c_\alpha$, one can easily obtain for $\nu_{\alpha\beta}$

$$\nu_{AA} = \nu(1 - 2\chi_{AS})$$
$$\nu_{BB} = \nu(1 - 2\chi_{BS})$$
$$\nu_{AB} = \nu(1 + \chi_{AB} - \chi_{AS} - \chi_{BS}) \quad \text{(A3)}$$

References and Notes

(1) Birshtein, T. M.; Borisov, O. V.; Zhulina, Y. B.; Khokhlov, A. R.; Yurasova, T. A. *Polym. Sci. USSR* **1987**, *29*, 1293.
(2) Wang, Z.-G.; Safran, S. A. *J. Chem. Phys.* **1988**, *89*, 5323.
(3) Fredrickson, G. H. *Macromolecules* **1993**, *26*, 2825.
(4) Rouault, Y.; Borisov, O. V. *Macromolecules* **1996**, *29*, 2605.
(5) Subbotin, A.; Saariaho, M.; Ikkala, O.; ten Brinke, G. *Macromolecules* **2000**, *33*, 3447.
(6) Subbotin, A.; Saariaho, M.; Stepanyan, R.; Ikkala, O.; ten Brinke, G. *Macromolecules* **2000**, *33*, 6168.
(7) Potemkin, I. I.; Khokhlov, A. R.; Reineker, P. *Eur. Phys. J. E* **2001**, *4*, 93.
(8) Stepanyan, R.; Subbotin, A.; ten Brinke, G. *Phys. Rev. E* **2001**, *63*, 061805.
(9) Saariaho, M.; Ikkala, O.; Szleifer, I.; Erukhimovich, I.; ten Brinke, G. *J. Chem. Phys.* **1997**, *107*, 3267.
(10) ten Brinke, G.; Ikkala, O. *TRIP* **1997**, *5*, 213.
(11) Rouault, Y. *Macromol. Theory Simul.* **1998**, *7*, 359.
(12) Saariaho, M.; Ikkala, O.; ten Brinke, G. *J. Chem. Phys.* **1999**, *110*, 1180.
(13) Saariaho, M.; Subbotin, A.; Szleifer, I.; Ikkala, O.; ten Brinke, G. *Macromolecules* **1999**, *32*, 4439.
(14) Saariaho, M.; Subbotin, A.; Ikkala, O.; ten Brinke, G. *Macromol. Rapid Commun.* **2000**, *21*, 110.
(15) Tsukahara, Y.; Mizuno, K.; Segawa, A.; Yamashita, Y. *Macromolecules* **1989**, *22*, 1546.
(16) Tsukahara, Y.; Tsutsumi, K.; Yamashita, Y. *Macromolecules* **1989**, *22*, 2869.
(17) Tsukahara, Y.; Tsutsumi, K.; Yamashita, S.; Shimada, S. *Macromolecules* **1990**, *23*, 5201.
(18) Tsukahara, Y. In *Macromolecular Design: Concept and Practice*; Mishra, M., Ed.; Polymer Frontiers International Inc.: New York, 1993.
(19) Beers, K. L.; Scott, G. G.; Mattyjaszewski, K.; Sheiko, S. S.; Möller, M. *Macromolecules* **1998**, *31*, 9413.
(20) Schappacher, M.; Billaud, C.; Paulo, C.; Deffieux, A. *Macromol. Chem. Phys.* **1999**, *200*, 2377.
(21) Börner, H. G.; Beers, K.; Matyjaszewski, K.; Sheiko, S. S.; Möller, M. *Macromolecules* **2001**, *34*, 4375.
(22) Wintermantel, M.; Schmidt, M.; Tsukahara, Y.; Kajiwara, K.; Kohjiya, S. *Macromol. Rapid Commun.* **1994**, *15*, 279.
(23) Wintermantel, M.; Fischer, K.; Gerle, M.; Ries, R.; Schmidt, M.; Kajiwara, K.; Urakawa, H.; Wataoka, I. *Angew. Chem., Int. Ed. Engl.* **1995**, *34*, 1472.
(24) Wintermantel, M.; Gerle, M.; Fischer, K.; Schmidt, M.; Wataoka, I.; Urakawa, H.; Kajiwara, K.; Tsukahara, Y. *Macromolecules* **1996**, *29*, 978.
(25) Dziezok, P.; Sheiko, S. S.; Fischer, K.; Schmidt, M.; Möller, M. *Angew. Chem., Int. Ed. Engl.* **1997**, *36*, 2812.
(26) Sheiko, S. S.; Gerle, M.; Fischer, F.; Schmidt, M.; Möller, M. *Langmuir* **1997**, *13*, 5368.
(27) Gerle, M.; Fischer, K.; Roos, S.; Müller, A. H. E.; Schmidt, M.; Sheiko, S. S.; Prokhorova, S.; Möller, M. *Macromolecules* **1999**, *32*, 2629.
(28) Fischer, K.; Gerle, M.; Schmidt, M. *Proc. ACS PMSE Anaheim* **1999**, *30*, 133.
(29) Helfand, E.; Wasserman, Z. R. *Macromolecules* **1976**, *9*, 879.
(30) Semenov, A. *Sov. Phys. JETP* **1985**, *61*, 733.
(31) Leibler, L. *Macromolecules* **1980**, *13*, 1602.

(32) Fredrickson, G. H.; Helfand, E. *Macromolecules* **1987**, *20*, 697.
(33) Dobrynin, A. V.; Erukhimovich, I. Y. *Macromolecules* **1993**, *26*, 276.
(34) Olvera de la Cruz, M.; Sanchez, I. *Macromolecules* **1986**, *19*, 2501.
(35) Foster, D. P.; Jasnow, D.; Balazs, A. C. *Macromolecules* **1995**, *28*, 3450.
(36) Werner, A.; Fredrickson, G. H. *J. Polym. Sci., Part B: Polym. Phys.* **1997**, *35*, 849.
(37) Nap, R. J.; Kok, C.; ten Brinke, G.; Kuchanov, S. I. *Eur. Phys. J. E* **2001**, *4*, 515.
(38) Semenov, A. N. *Macromolecules* **1993**, *26*, 2273.
(39) Grosberg, A. Yu.; Khokhlov, A. R. *Statistical Physics of Macromolecules*; American Institute of Physics: New York, 1994.
(40) Milner, S. T.; Wang, Z.-G.; Witten, T. A. *Macromolecules* **1989**, *22*, 489.
(41) de Gennes, P.-G. *Scaling Concepts in Polymer Physics*; Cornell University Press: Ithaca, NY, 1985.
(42) Ball, R. C.; Marko, J. F.; Milner, S. T.; Witten, T. A. *Macromolecules* **1991**, *24*, 693.
(43) Lai, H.; Witten, T. A. *Macromolecules* **1991**, *24*, 693.
(44) des Cloizeaux, J.; Jannink, G. *Polymers in Solutions: Their Modelling and Structure*; Clarendon Press: Oxford, 1990.
(45) Joanny, J.-F.; Leibler, L.; Ball, R. *J. Chem. Phys.* **1984**, *81*, 4640.
(46) Schäfer, L.; Kappeler, Ch. *J. Phys. (Paris)* **1985**, *46*, 1853.
(47) Schaefer, D. W.; Joanny, J. F.; Pincus, P. *Macromolecules* **1980**, *13*, 1280.
(48) Odijk, T. *J. Polym. Sci., Polym. Phys. Ed.* **1977**, *15*, 477.
(49) Skolnick, J.; Fixmann, M. *Macromolecules* **1977,** *10*, 944.
(50) Khalatur, P. G.; Khokhlov, A. R.; Prokhorova, S. A.; Sheiko, S. S.; Möller, M.; Reineker, P.; Shirvanyanz, D. G.; Starovoitova, N. *Eur. Phys. J. E* **2000**, *1*, 99.
(51) Vasilevskaya, V. V.; Khokhlov, A. R.; Kidoaki, S.; Yoshikawa, K. *Biopolymers* **1997**, *41*, 51.

MA011441L